Glycine amide shielding on the aromatic surfaces of lysozyme: Implication for suppression of protein aggregation

Len Ito,[a] Kentaro Shiraki,[b] Masatomo Makino,[a] Kazuya Hasegawa,[a] and Takashi Kumasaka [a]

[a]*Japan Synchrotron Radiation Research Institute (SPring-8), 1-1-1 Kouto, Sayo, Hyogo 679-5198, Japan*
[b]*Institute of Applied Physics, University of Tsukuba, 1-1-1 Tennodai, Tsukuba, Ibaraki 305-8573, Japan*

[*]Corresponding author: Japan Synchrotron Radiation Research Institute, 1-1-1 Kouto, Sayo, Hyogo 679-5198, Japan Tel.: +81-791-58-0833; Fax: +81-791-58-0830
E-mail address: l-ito@spring8.or.jp (L. Ito)

Keywords: glycine amide; crystal structure; lysozyme; protein aggregation; accessible surface area

Abstract

Glycine amide (GlyAd), a typically amidated amino acid, is a versatile additive that suppresses protein aggregation during refolding, heat treatment, and crystallization. In spite of its effectiveness, the exact mechanism by which GlyAd suppresses protein aggregation remains to be elucidated. Here, we show the crystal structure of the GlyAd–lysozyme complex by high resolution X-ray crystallographic analysis at a 1.05 Å resolution. GlyAd bound to the lysozyme surface near aromatic residues and decreased the amount of bound waters and increased the mobility of protein. Arg and GlyAd molecules are different in binding sites and patterns from glycerol and related compounds, indicating that decreasing hydrophobic patches might be involved in suppression of protein aggregation.

1. Introduction

Control of protein aggregation is a crucial method for biotechnological and medical applications of proteins. To prevent protein aggregation, the addition of small molecules into the protein solution is often used as a convenient approach [1-4]. Briefly, the solution additives can be classified into two types, protein stabilizers and protein destabilizers [5]. Protein stabilizers are typically classified into kosmotropes such as ammonium sulfate and sugars, [6-8] and into macromolecular crowding agents such as polyols and polysaccharides [9-12]. These additives generally stabilize the native state molecules. However, they often accelerate protein aggregation. Protein destabilizers such as urea and guanidine hydrochloride (Gdn-HCl) are typically classified as chaotropes. These additives mostly denature proteins at higher concentrations. Furthermore, these additives weaken the intermolecular hydrophobic interactions of proteins at non-denaturing concentrations, leading to suppression of aggregation during refolding and heating [13-15].

Among these additives, arginine (Arg) has been widely used in biochemical studies to increase refolding yields by decreasing aggregation [1, 2, 4, 11, 16-23]. Amino acid derivatives such as amidated and alkyl ethyl esterified amino acids are more effective additives than Arg for both heat-induced and refolding-induced aggregation of lysozyme [24-26]. In particular, the amidated amino acids are ideal additives because they are stable at neutral pH as

compared with alkyl ethyl estered amino acids, which are easily hydrolyzed. Furthermore, of all the amino acids and their derivatives, glycine amide (GlyAd) is the most favorable additive for suppressing the aggregation of proteins in saturated protein solutions, and increasing the probability of crystal formation of proteins [27].

Despite its effectiveness, the molecular mechanisms of amino acids and amino acid derivatives are unclear. A suggested mechanism is that chaotropes alter the stability of proteins by directly binding to them, resulting in weakening of hydrophobic interactions [27-29]. Previously, we reported the crystallization conditions in the presence of these molecules [30]. We are trying to analyze the crystal structure of protein complex with these molecules, such as Arg, GlyAd, GlyEE, and amino acids. It is difficult to analyze these crystal structures because of lower occupancy of these molecules. However, we showed that high resolution of crystallographic analysis was effective in the analysis of Arg [31]. Now, we successfully determined the high-resolution crystal structures of the lysozyme complex with GlyAd. As a result, we showed the specific binding of GlyAd on a protein surface as a characteristic of an aggregation suppressor.

2. Materials and Methods

2.1. Reagents

GlyAd and all chemicals of high quality and analytical grade were purchased from Wako Pure Chemical Industries (Osaka, Japan). Six times recrystallized egg-white lysozyme (HEWL) was purchased from Seikagaku-Kogyo Co. (Tokyo, Japan).

2.2. Turbidity measurement

The HEWL solubility in the presence of three types of precipitants, sodium chloride, ethanol, and polyethylene glycol (PEG) 4000, were measured by the turbidity of the solution. The stock solutions of the precipitants were prepared as follows. Solutions containing 11 different sodium chloride concentrations (2.2, 2.4, 2.6, 2.8, 3.0, 3.2, 3.4, 3.6, 3.8, 4.0, and 4.2 M), seven different ethanol concentrations (70%, 75%, 80%, 85%, 90%, 95%, and 100%), and seven different PEG 4000 concentrations (30%, 35%, 40%, 45%, 50%, 55%, and 60%) were prepared in 0.1 M sodium acetate (pH 4.5).

A stock protein solution containing 20 mg/mL lysozyme was prepared in 0.1 M sodium acetate (pH 4.5) in the presence and absence of 400 mM Gly or GlyAd. Stock precipitant solutions were adjusted to pH 4.5 before mixing with the protein solutions and filtered through disposable 0.2-μm sterile syringe filters. Each

measurement sample was obtained by mixing 500 μL of the protein solution with an equal volume of each precipitant solution in a 1.5-mL microtube. After two days, the turbidity of the mixture was measured at 600 nm using a Jasco spectrophotometer, model V-550 (Jasco Co., Tokyo, Japan). Experimental reproducibility was evaluated by repeating each experiment more than three times.

2.3. Crystallization

Crystallization of HEWL in the presence of GlyAd was performed as follows. A protein solution containing 150 mg mL^{-1} HEWL in 0.1 M sodium acetate buffer at pH 4.5 was prepared in a 1.5-mL microtube. The concentration of protein was measured by absorbance at 280 nm using a ND-1000 UV-Vis spectrophotometer (NanoDrop Technologies, Wilmington, DE, USA) and the extinction coefficient of 2.63 mL mg^{-1} cm^{-1} [32]. The batch method was used for crystallization at 20°C. Droplets were prepared by mixing 1.5 μL of protein solution with an equal amount of a solution containing 2.0 M GlyAd and 0.1 M sodium acetate buffer at pH 4.5.

2.4. Data collection and determination of crystal structures

X-ray diffraction data were collected from the GlyAd-lysozyme crystal on beamline BL32B2 at SPring-8 using a Rigaku R-AXIS V

imaging plate detector. The diffraction data set was collected under cryogenic conditions from the crystal soaked in paratone-N (Hampton Research Co., CA, USA) and cooled at −173°C in a cold nitrogen gas stream. The diffraction images were taken at an oscillation angle of 0.5° and exposure times of 3.0 s. The data were integrated at 50–1.05 Å resolution and then scaled using the *HKL-2000* program package [33]. Restrained refinement of the lysozyme structure (PDBID: 193L) in *REFMAC* [34], and *ARP/wARP v.7.1* [35] in the *CCP4* suite [36], was used for the refinement and the addition of water molecules to the model, respectively. Molecular modeling by manual fitting to the electron density map was performed using the *COOT* program [37]. In the case of the crystal obtained from the solution containing GlyAd, the cross-validated σ_A-weighted $2|F_o| - |F_c|$ and $|F_o| - |F_c|$ electron density maps clearly revealed the residual electron densities corresponding to four GlyAd molecules (GlyAd 1–4). The average isotropic temperature factors and occupancy of GlyAd are 27.6 Å^2 and 0.51, 16.7 Å^2 and 1.0, 12.4 Å^2 and 1.0, and 12.7 Å^2 and 1.0 for GlyAd 1, GlyAd 2, GlyAd 3, and GlyAd 4, respectively. The GlyAd occupancy refinement was performed using the *PHENIX* program [38]. The value of the average *B*-factor of the protein was 12.7 Å^2. The root mean square deviations from the ideal geometry were 0.20 Å for the bond length and 2.0° for the bond angles. The crystal data and relevant statistics are shown in Table 1. All figures were prepared using the program *PyMOL* [39].

2.5. Intrinsic fluorescence measurements

Intrinsic fluorescence emission spectra of proteins were obtained at an excitation wavelength of 295 nm with a 10-nm slit width using an RF-1500 fluorescence spectrophotometer (Shimadzu Co., Kyoto, Japan) at 20°C. Fluorescence spectra were recorded for 0.3 mg mL^{-1} protein in 0.1 M sodium acetate buffer (pH 4.5). The spectra of samples were corrected by subtracting the corresponding buffers' spectra.

3. Results and discussion

3.1. Turbidity Measurements.

Turbidities of the lysozyme solutions containing different concentrations of sodium chloride (a), ethanol (b), and PEG4000 (c) were evaluated by optical density at 600 nm in the presence or absence of 0.2 M Gly or GlyAd at pH 4.5 as shown in Figure 1. The turbidity steeply increased with increasing concentrations of sodium chloride at around 1.9 M. In the presence of Gly, the turbidity increased similarly, i.e. at around 1.7 M NaCl (Fig. 1a). The turbidity also increased with increasing concentration of ethanol and PEG4000. In these cases, Gly decreased the turbidity development,

indicating that Gly weakly suppresses protein aggregation. With increasing concentrations of sodium chloride, ethanol, and PEG 4000, the turbidity decreased in the presence of GlyAd as compared with the experiments in the absence or presence of Gly. This indicates that GlyAd inhibits aggregation of lysozyme in various types of supersaturated solution. Recently, we reported improvement in the success rate of crystallization using commercially available screen kits with the usage of GlyAd as an additive [40]. High ionic strength such as sodium chloride (Fig. 1a) can weaken hydrogen bonding and ionic interactions, but may enhance hydrophobic interactions [41, 42]. Conversely, organic solvents such as ethanol and PEG (Fig. 1b and c) can weaken hydrophobic interactions, but may strengthen hydrogen bonding and ionic interactions [43]. As expected, GlyAd decreased protein aggregation in the various types of saturated solutions as well as increased the probability of obtaining protein crystals. However, the structural mechanism of GlyAd for suppression of protein aggregation is not known. The X-ray crystallographic data of the GlyAd-lysozyme complex are described in the following sections.

3.2. Interaction of GlyAd with Lysozyme.

Figure 2a shows the ribbon model of the main chain and stick model of the side chains of Glu 35, Asp 52, six Trp residues (residue

numbers: 28, 62, 63, 108, 111, and 123) of lysozyme, and binding of four GlyAd molecules. These bound GlyAd molecules were observed at four binding sites on the protein surface, with a result of reasonable occupancy (Fig. 2b). GlyAd 2 binding site was formed on the residue of Asn 44 (Fig. 2e). GlyAd 3 binding site was located on Phe 34 and Glu 35 (Fig. 2e). GlyAd 4 binding site was located on Gln 57, Asn 59, Ala 107, and Trp 108 nearby active sites (Fig. 2d). GlyAd 1 binding site directly interacted with the aromatic side chain of Trp 62 at the substrate-binding site of lysozyme and was formed by the side chain of Asp 101 (Fig. 2c). Almost all the binding structures showed similar patterns where the carbonyl amide, amino groups, and carbonyl O of GlyAd formed hydrogen bonds with side chains of lysozyme and a few water molecules as shown in Table 2. In particular, the carbonyl amide of GlyAd formed a number of hydrogen bonds with water and the lysozyme surface.

Our recent results on the high resolution crystal structure of the Arg-lysozym e complex showed that Arg directly or indirectly bound to aromatic residues of lysozyme and their occupancies gradually increased with increasing Arg concentration [31]. These interactions between the guanidino group of Arg and lysozyme are mediated by electrostatic contacts, hydrophobic contacts, and the cation-π interactions with the surface residues, but the main chain of Arg was disordered. On the other hand, the binding sites of GlyAd were different from the binding sites of Arg, thus almost all of the

bound GlyAd formed only hydrogen bonds between the carbonyl amide group and the surface residues of lysozyme and hydrated water.

To evaluate the effects of GlyAd, we compared our structure and the high resolution structure of GlyAd-free native lysozyme (PDB-ID: 3LZT). Our structure contains the only one half the hydrated water molecules of the GlyAd-free structure (GlyAd, 175 waters; 3LZT, 347 waters). The differences in average temperature factor between the two structures was 4.2 $Å^2$ for protein and –1.4 $Å^2$ for water, respectively, indicating that GlyAd increases the mobility of lysozyme and decreases the mobility of water molecules. In general, chaotropes such as Arg and GlyAd break down the hydrogen-bonded network of water, so rendering macromolecules more mobile and encouraging protein expansion and denaturation. Our study showed the properties of GlyAd typical as a chaotrope. Furthermore, we examined the other molecules resolved in lysozyme crystal structures: lysozyme-MPD complex (PDBID: 1DPW), lysozyme-nitrate ion complex (PDBID: 3LZT), and lysozyme-ethylene glycol complex (PDBID: 2VB1). Although all the small molecules preferentially bind around the active site cleft, GlyAd and Arg show different binding patterns. While GlyAd and Arg directly or indirectly bind to aromatic residues as described, the other molecules directly bind to hydrophobic residues and hydrated waters with hydrogen bond, but not aromatic residues. The preferential

binding of Arg and GlyAd to hydrophobic surface patch of Arg and GlyAd might decrease the probability of protein aggregation and it is consistent with our previous reports.

Matsuoka et al. attempted to classify the effects of various additive compounds for understanding the mechanism to suppress protein aggregation [25]. However, it is still unclear in their study whether Arg and amidated amino acid molecules bind to the protein surfaces. Our findings showed that the specific interactions of the carbonyl amide and amino groups of GlyAd are due to thermodynamic (equilibrium) binding of the amidated additives with the proteins. Our crystal structure showed that GlyAd specifically binding to the surfaces of hydrophobic region, especially near aromatic amino acid residues might increase the apparent net charge of the aggregation-prone molecules, leading to increased electrostatic repulsion. Our data support these findings by showing that the amount of aggregation gradually increased with increasing concentration of sodium chloride as shown Figure 1a. These results suggest that high concentrations of sodium chloride may disrupt the electrostatic interactions between the lysozyme surface and GlyAd.

3.3. Effects of GlyAd on Intrinsic Fluorescence.

Lysozyme has six Trp residues (Fig. 2). Almost all (80%) of the intrinsic fluorescence of lysozyme is due to Trp 62 and Trp 108

[44]. Figure 3 shows the fluorescence spectrum of lysozyme in 0.1 M sodium acetate buffer (pH 4.5) excited at 295 nm. The emission spectrum showed a broad peak at 339 nm in the absence of the additive, while a slight blue shift to 337 nm was observed, along with decreased emission intensity by 7% and 23% in the presence of 1.0 M sodium chloride and 1.0 M GlyAd, respectively. The effects of GlyAd may be due to the binding of GlyAd to Trp 62 and 108 [44], which is consistent with the structural data as described later (Fig. 2c–e).

3.4. Comparison of Accessible Surface Areas of the GlyAd-Complex with Lysozyme Alone.

All of the bound GlyAd molecules were in close proximity to the aromatic amino acid residues, Trp 62 and Trp 63 (GlyAd 1: Fig. 2c), Phe 34 (GlyAd 3: Fig. 2e), and Trp 108 (GlyAd 4: Fig. 2d). Table 3 lists the data for the accessible surface areas (ASAs) of the GlyAd-lysozyme complex and lysozyme structures (PDB ID: 1HEL, 193L, 1BWH, 1BVM, and 1QTK) with *AREAIMOL* in the *CCP4* suite. The ASA of the GlyAd-lysozyme complex (6530 $Å^2$) was slightly larger than that of lysozyme alone (6455 ± 73 $Å^2$) due to the binding of GlyAds to the small cavities of the protein surface. The contributions of hydrophobic, polar, and charged residues to the total ASA were analyzed in the crystal structures as shown in Table 3.

Although no significant difference was obtained in the polar residue composition between the two structures, the ASA of the aromatic amino acid residues drastically decreased by 29.0% and the ASA of the charged amino acid residues including GlyAd increased by 16.3% as compared with that of lysozyme alone. In particular, GlyAd-lysozyme exposes less aromatic hydrophobic residues and more charged residues to the solvent by binding of GlyAd. The direct binding of chaotropic molecules to proteins may result in further weakening of the hydrophobic interactions between non-polar amino acids that stabilize the native state of proteins [28]. Turbidity measurement showed that addition of GlyAd decreased protein aggregation using ethanol and PEG (Fig. 1b and c). These results imply decreasing ASA of the aromatic side chains (Fig. 1a) and increasing ASA of the charged side chains (Fig. 1b and c) in the presence of GlyAd molecules and gives insight into how GlyAd prevents protein aggregation.

4. Conclusion

This study focused on the structural basis, determined by high resolution X-ray crystallographic analysis, for the decrease in protein aggregation by addition of GlyAd. It is evident that GlyAd binds to protein surface near aromatic residues. The behavior of GlyAd is

similar to arginine as an additive for use in protein solutions. The evidence presented in the present study suggests a mechanism for suppression of protein aggregation in the presence of GlyAd and other additives.

Acknowledgement

This work was supported by the Sasagawa Scientific Research Grant from the Japan Science Society.

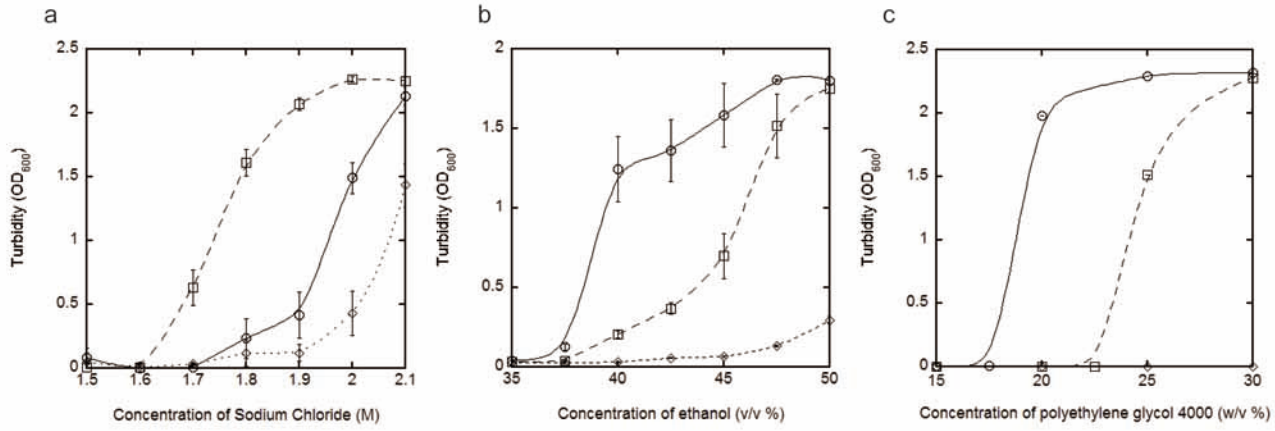

Figure 1. Aggregation of lysozyme in various concentrations of sodium chloride (a), ethanol (b), and polyethylene glycol 4000 (c) in the presence or absence of Gly and GlyAd at pH 6.5. The aggregation was monitored by turbidity at 600 nm and 20°C. No additive, circles; Gly, squares; 0.2 M GlyAd, rhomboid.

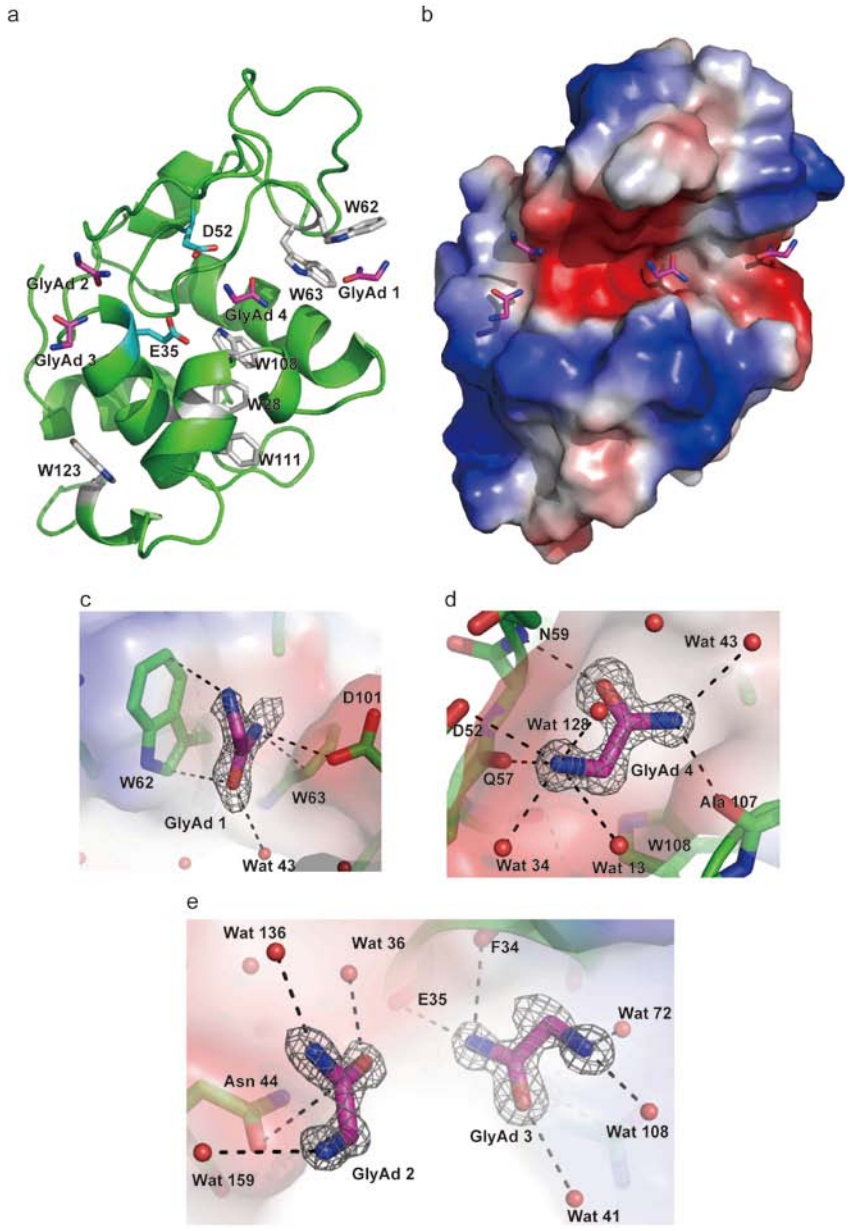

Figure 2. (a) The GlyAd-lysozyme ribbon model, green; the active site of Glu 35 and Asp 52, cyan; GlyAd molecules, magenta; Trp residues, silver. (b) Surface charge potential of lysozyme. The maps are contoured at $F_o - F_c = 2.5\ \sigma$ (c, GlyAd 1), 4.0 σ (d, GlyAd 4), and 4.0 σ (e, GlyAd 2 and GlyAd 3).

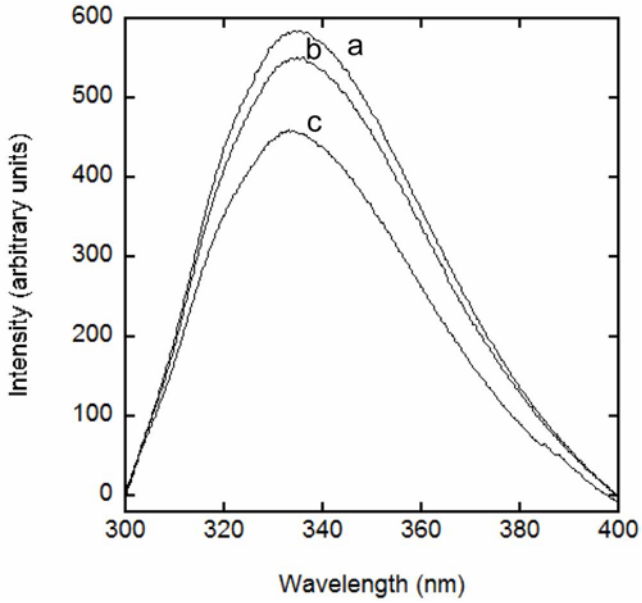

Figure 3. Intrinsic emission fluorescence spectra of lysozyme. The samples consisted of 0.3 mg·mL^{-1} lysozyme alone (a), in the presence of 1.0 M NaCl (b), and 1.0 M GlyAd (c) in 0.1 M sodium acetate pH 4.5 at 20°C. The excitation wavelength was 295 nm.

Data collection	
Beam line	BL32B2 (SPring−8)
Detector	R-AXIS V (Rigaku)
Wavelength (Å)	1.000
Crystal- to- detector distance (mm)	150.0
Oscillation angle (°)	0.5
Exposure time (s frame-1)	3.0
Total oscillation range (°)	180
Space group	$P4_32_12$
Unit cell parameters	
a (Å)[a]	78.51
c (Å)[a]	36.96
Resolution (Å)[b]	50-1.05 (1.09−1.05)
Unique reflections[b]	102269 (9704)
Redundancy[b]	6.8 (3.5)
Completeness (%)[b]	99.3 (94.0)
R_{merge}[b, c]	0.039 (0.308)
$I/\sigma(I)$[b]	68.7 (5.5)
Refinement	
Resolution limits (Å)[b]	30.0-1.05 (1.08−1.05)
R_{factor}[b, d]	0.146 (0.196)
R_{free}[b, e]	0.163 (0.212)
R.m.s.d. bond lengths (Å)	0.020
R.m.s.d. bond angles (°)	2.0
PDB ID	3AJN

Table 1. Data-collection and refinement statistics.

[a]The values in parentheses are the average values of unit cell dimensions. [b]The values in parentheses are for reflections in the highest resolution shell. [c]$R_{merge} = \Sigma|I_i - \langle I \rangle|\Sigma I_i$, where I_i is the intensity of the i[th] observation and $\langle I \rangle$ is the mean intensity of the reflection. [d]$R_{factor} = \Sigma||F_{obs}| - |F_{calc}||/\Sigma|F_{obs}|$. R_{free} is equivalent to R, but is calculated using a test set of reflections excluded from the final refinement stages.

Substrate	Atom	Residue	Atom	Distance (Å)	Substrate	Atom	Residue	Atom	Distance (Å)
GlyAd 1	N2	Trp 62	CZ3	3.47	GlyAd 3	C	Wat 72	O	3.34
GlyAd 1	N2	Trp 62	CH2	3.49	GlyAd 3	O	Asn 37	CB	3.49
GlyAd 1	C	Asp101	CD2	3.40	GlyAd 3	O	Wat 41	O	3.06
GlyAd 1	O	Wat 43	O	3.47	GlyAd 3	N1	Glu 35	C	3.36
GlyAd 1	O	Trp 62	CD1	3.43	GlyAd 3	N1	Phe 34	O	2.98
GlyAd 1	N1	Trp 62	CG	3.46	GlyAd 3	N1	Glu 35	O	3.14
GlyAd 1	N1	Trp 62	CD2	3.41					
GlyAd 1	N1	Trp 63	CZ2	3.47					
GlyAd 1	N1	Asp 101	OD2	3.35	GlyAd 4	N2	Wat 13	O	3.45
					GlyAd 4	N2	Gln 57	O	2.64
GlyAd 2	N2	Wat 159	O	3.42	GlyAd 4	N2	Wat 34	O	2.82
GlyAd 2	CA	Asn 44	OD1	3.30	GlyAd 4	N2	Asp 52	OD1	3.21
GlyAd 2	C	Asn 44	OD1	3.41	GlyAd 4	N2	Wat 128	O	2.93
GlyAd 2	O	Wat 36	O	2.96	GlyAd 4	CA	Gln 57	O	3.21
GlyAd 2	N1	Wat 136	O	2.88	GlyAd 4	CA	Wat 128	O	3.45
					GlyAd 4	C	Wat 128	O	3.46
GlyAd 3	N2	Wat 72	O	2.75	GlyAd 4	O	Asn 59	CB	3.29
GlyAd 3	N2	Wat 108	O	2.78	GlyAd 4	O	Asn 59	N	2.91
GlyAd 3	CA	Wat 72	O	2.54	GlyAd 4	N1	Ala 107	O	2.93
GlyAd 3	CA	Phe 34	O	3.27	GlyAd 4	N1	Wat 43	O	3.22

Table 2. Distances between atoms in GlyAd 1–4 and lysozyme as judged by the distances from 2.1 to 3.5 Å.

	GlyAd-lysozyme Comple›	lysozyme Alone	ASA of Complex/Alone (%)
Total ASA (Å^2)	6530	6455±73	1.2
ASA hydrophobic residues (Å^2)	1374	1529±25	-10.2
ASA aromatic residues (Å^2)	305.0	430±8	-29.0
ASA polar residues (Å^2)	1888	1948±29	-3.1
ASA charged residues (Å^2)	2964	2548±35	16.3

Table 3. Comparison of ASAs between the GlyAd-lysozyme complex and average and variance of lysozyme alone (PDBID: 1HEL, 193L, 1IEE, 1BWH, 1LJN, 1BVM, and 1QTK)

References

1. Shiraki K, Kudou M, Fujiwara S, Imanaka T & Takagi M (2002) Biophysical effect of amino acids on the prevention of protein aggregation. *J Biochem* **132**, 591-595.

2. Shiraki K, Kudou M, Nishikori S, Kitagawa H, Imanaka T & Takagi M (2004) Arginine ethylester prevents thermal inactivation and aggregation of lysozyme. *Eur J Biochem* **271**, 3242-3247.

3. Tsumoto K, Shinoki K, Kondo H, Uchikawa M, Juji T & Kumagai I (1998) Highly efficient recovery of functional single-chain Fv fragments from inclusion bodies overexpressed in Escherichia coli by controlled introduction of oxidizing reagent--application to a human single-chain Fv fragment. *J Immunol Methods* **219**, 119-129.

4. Tsumoto K, Umetsu M, Kumagai I, Ejima D & Arakawa T (2003) Solubilization of active green fluorescent protein from insoluble particles by guanidine and arginine. *Biochem Biophys Res Commun* **312**, 1383-1386.

5. Tsumoto K, Ejima D, Kumagai I & Arakawa T (2003) Practical considerations in refolding proteins from inclusion bodies. *Protein Expr Purif* **28**, 1-8.

6. Eronina TB, Chebotareva NA & Kurganov BI (2005) Influence of osmolytes on inactivation and aggregation of muscle glycogen phosphorylase b by guanidine hydrochloride. Stimulation of protein aggregation under crowding conditions. *Biochemistry (Mosc)* **70**, 1020-1026.

7. Hirano A, Hamada H, Okubo T, Noguchi T, Higashibata H & Shiraki K (2007) Correlation between thermal aggregation and stability of lysozyme with salts described by molar surface tension increment: an exceptional propensity of ammonium salts as aggregation suppressor. *Protein J* **26**, 423-433.

8. Maeda Y, Yamada H, Ueda T & Imoto T (1996) Effect of additives on the renaturation of reduced lysozyme in the presence of 4 M urea. *Protein Eng* **9**, 461-465.

9. Dong XY, Huang Y & Sun Y (2004) Refolding kinetics of denatured-reduced lysozyme in the presence of folding aids. *J Biotechnol* **114**, 135-142.

10. Haque I, Islam A, Singh R, Moosavi-Movahedi AA & Ahmad F (2006) Stability of proteins in the presence of polyols estimated from their guanidinium chloride-induced transition curves at different pH values and 25 degrees C. *Biophys Chem* **119**, 224-233.

11. Meng F, Park Y & Zhou H (2001) Role of proline, glycerol, and heparin as protein folding aids during refolding of rabbit muscle creatine kinase. *Int J Biochem Cell Biol* **33**, 701-709.

12. Sasahara K, McPhie P & Minton AP (2003) Effect of dextran on protein stability and conformation attributed to macromolecular crowding. *J Mol Biol* **326**, 1227-1237.

13. Arakawa T & Timasheff SN (1984) Protein stabilization and destabilization by

guanidinium salts. *Biochemistry* **23**, 5924-5929.

14. Bhuyan AK (2002) Protein stabilization by urea and guanidine hydrochloride. *Biochemistry* **41**, 13386-13394.

15. Orsini G & Goldberg ME (1978) The renaturation of reduced chymotrypsinogen A in guanidine HCl. Refolding versus aggregation. *J Biol Chem* **253**, 3453-3458.

16. Shiraki K, Kudou M, Sakamoto R, Yanagihara I & Takagi M (2005) Amino Acid esters prevent thermal inactivation and aggregation of lysozyme. *Biotechnol Prog* **21**, 640-643.

17. Arakawa T & Tsumoto K (2003) The effects of arginine on refolding of aggregated proteins: not facilitate refolding, but suppress aggregation. *Biochem Biophys Res Commun* **304**, 148-152.

18. Umetsu M, Tsumoto K, Hara M, Ashish K, Goda S, Adschiri T & Kumagai I (2003) How additives influence the refolding of immunoglobulin-folded proteins in a stepwise dialysis system. Spectroscopic evidence for highly efficient refolding of a single-chain Fv fragment. *J Biol Chem* **278**, 8979-8987.

19. Taneja S & Ahmad F (1994) Increased thermal stability of proteins in the presence of amino acids. *Biochem J* **303 (Pt 1)**, 147-153.

20. Brinkmann U, Buchner J & Pastan I (1992) Independent domain folding of Pseudomonas exotoxin and single-chain immunotoxins: influence of interdomain connections. *Proc Natl Acad Sci U S A* **89**, 3075-3079.

21. Buchner J & Rudolph R (1991) Renaturation, purification and characterization of recombinant Fab-fragments produced in Escherichia coli. *Biotechnology (N Y)* **9**, 157-162.

22. Samuel D, Kumar TK, Ganesh G, Jayaraman G, Yang PW, Chang MM, Trivedi VD, Wang SL, Hwang KC, Chang DK, et al. (2000) Proline inhibits aggregation during protein refolding. *Protein Sci* **9**, 344-352.

23. Kumar TK, Samuel D, Jayaraman G, Srimathi T & Yu C (1998) The role of proline in the prevention of aggregation during protein folding in vitro. *Biochem Mol Biol Int* **46**, 509-517.

24. Hamada H & Shiraki K (2007) L-argininamide improves the refolding more effectively than L-arginine. *J Biotechnol* **130**, 153-160.

25. Matsuoka T, Hamada H, Matsumoto K & Shiraki K (2009) Indispensable structure of solution additives to prevent inactivation of lysozyme for heating and refolding. *Biotechnol Prog* **25**, 1515-1524.

26. Matsuoka T, Tomita S, Hamada H & Shiraki K (2007) Amidated amino acids are prominent additives for preventing heat-induced aggregation of lysozyme. *J Biosci Bioeng* **103**, 440-443.

27. Timasheff SN (2002) Protein-solvent preferential interactions, protein hydration, and the modulation of biochemical reactions by solvent components. *Proc Natl Acad Sci U S A* **99**, 9721-9726.

28. Salvi G, De Los Rios P & Vendruscolo M (2005) Effective interactions between chaotropic agents and proteins. *Proteins* **61**, 492-499.

29. Bennion BJ & Daggett V (2003) The molecular basis for the chemical denaturation of proteins by urea. *Proc Natl Acad Sci U S A* **100**, 5142-5147.

30. Ito L, Shiraki K & Yamaguchi H (2010) Amino acids and glycine ethyl ester as new crystallization reagents for lysozyme. *Acta Crystallographica Section F* **66**, 750-754.

31. Ito L, Shiraki K, Matsuura T, Okumura M, Hasegawa K, Baba S, Yamaguchi H & Kumasaka T High-resolution X-ray analysis reveals binding of arginine to aromatic residues of lysozyme surface: implication of suppression of protein aggregation by arginine. *Protein Eng Des Sel*. in press.

32. Saxena VP & Wetlaufer DB (1970) Formation of three-dimensional structure in proteins. I. Rapid nonenzymic reactivation of reduced lysozyme. *Biochemistry* **9**, 5015-5023.

33. Otwinowski Z, Minor W & Charles W. Carter, Jr. (1997) [20] Processing of X-ray diffraction data collected in oscillation mode. In *Methods in Enzymology*, pp. 307-326. Academic Press.

34. Murshudov GN, Vagin AA & Dodson EJ (1997) Refinement of macromolecular structures by the maximum-likelihood method. *Acta Crystallogr D Biol Crystallogr* **53**, 240-255.

35. Perrakis A, Morris R & Lamzin VS (1999) Automated protein model building combined with iterative structure refinement. *Nat Struct Biol* **6**, 458-463, doi: 10.1038/8263.

36. Collaborative Computational Project N (1994) The CCP4 suite: programs for protein crystallography. *Acta Crystallographica Section D* **50**, 760-763.

37. Emsley P & Cowtan K (2004) Coot: model-building tools for molecular graphics. *Acta Crystallogr D Biol Crystallogr* **60**, 2126-2132.

38. Adams PD, Grosse-Kunstleve RW, Hung LW, Ioerger TR, McCoy AJ, Moriarty NW, Read RJ, Sacchettini JC, Sauter NK & Terwilliger TC (2002) PHENIX: building new software for automated crystallographic structure determination. *Acta Crystallogr D Biol Crystallogr* **58**, 1948-1954.

39. DeLano,W.L. The PyMOL Molecular Graphics System. DeLano Scientific, San Carlos, CA. http://www.pymol.org.

40. Ito L, Shiraki K & Yamaguchi H (2010) Comparative analysis of amino acids and amino-acid derivatives in protein crystallization. *Acta Crystallographica Section F* **66**, 744-749.

41. Rimerman RA & Hatfield GW (1973) Phosphate-induced protein chromatography. *Science* **182**, 1268-1270.

42. Shaltiel S & Er-El Z (1973) Hydrophobic chromatography: use for purification of glycogen synthetase. *Proc Natl Acad Sci U S A* **70**, 778-781.

43. Gekko K, Ohmae E, Kameyama K & Takagi T (1998) Acetonitrile-protein interactions: amino acid solubility and preferential solvation. *Biochim Biophys Acta* **1387**, 195-205.

44. Imoto T, Forster LS, Rupley JA & Tanaka F (1972) Fluorescence of lysozyme: emissions from tryptophan residues 62 and 108 and energy migration. *Proc Natl Acad Sci U S A* **69**, 1151-1155.